Supporting Information

$MoSe_2$-Based Room Temperature Gas Sensor with Sub-parts-per-billion Limit of Ammonia and N, N-Dimethylformamide

Virendra Singh Choudhary[a], Ramandeep[a], Ashok Kumar[a], C. S. Yadav[b], Sandeep Sharma[d], Joel Garcia[c#], Surender Kumar Sharma[a*]

[a]Department of Physics, School of basic Sciences, Central University of Punjab, Bathinda-151401, India

[b]Department of Physics, Indian Institute of Technology, Mandi, 175075, India

[c]Department of Chemistry, De La Salle University, Manila, Philippines

[d]Department of Physics and Photonics Science, National Institute of Technology, Hamirpur, Himachal Pradesh-177005, India

[#, *] Email: joel.garcia@dlsu.edu.ph; surender.sharma@cup.edu.in

The supporting information contains:
Total Number of Pages: 10
Total Number of Figures: 13
Total Number of Tables: 2

Table S1: Performance comparison of various NH_3 and DMF sensors in the present work.

Materials	Response	Analytes (Con.)	Humidity/ Temp. (deg	$t_{response}/t_{recovery}$	LOD	ref
$MoSe_2$	2%	10 ppm (NH_3)	RT	13/140	No	1
Single-layer MoSe2	13%	500 ppm (NH_3)	RT	150/540	No	2
Au-MoSe2 composite	2.6%	20 ppm (NH_3)	RT	18/16	No	3
Nb doped-$MoSe_2$	8%	3 ppm (NH_3)	150°C	30/1800	No	4
Pd NPs/TiO_2/rGO	1.18%	10 ppm (NH_3)	RT	184/81	No	5
MoS_2/CuO	47%	100 ppm (NH_3)	RT	17/26	No	6
MoS_2/WO_3	207%	200 ppm (NH_3)	200	80/70	No	7
WS_2/TiO_2	43%	250 ppm (NH_3)	RT	200/...	No	8
$MoSe_2$/MoO_3	10%	10 ppm (DMF)	55% / RT	135/216	No	9
$MoSe_2$/rGO	3.6%	2 ppm (DMF)	RT	130/50	No	10
$MoSe_2$/TiO_2 (2:1)	**1%**	**1 ppm(NH_3) & 3 ppm (DMF)**	**RT**	**150/37 (NH3) 150/45 (DMF)**	**4.91 ppb & 7.82 ppb**	**This Work**

Table S2: Details of $MoSe_2$, TiO_2, and $MoSe_2$-TiO_2 composite samplessynthesized at different weight ratio.

Sr No.	Device Name	Sample ID	Weight ratio
1	MS	$MoSe_2$	1
2	TO	TiO_2	1
3	MT11	$MoSe_2$/TiO_2	1:1
4	MT12	$MoSe_2$/TiO_2	1:2
5	MT21	$MoSe_2$/TiO_2	2:1

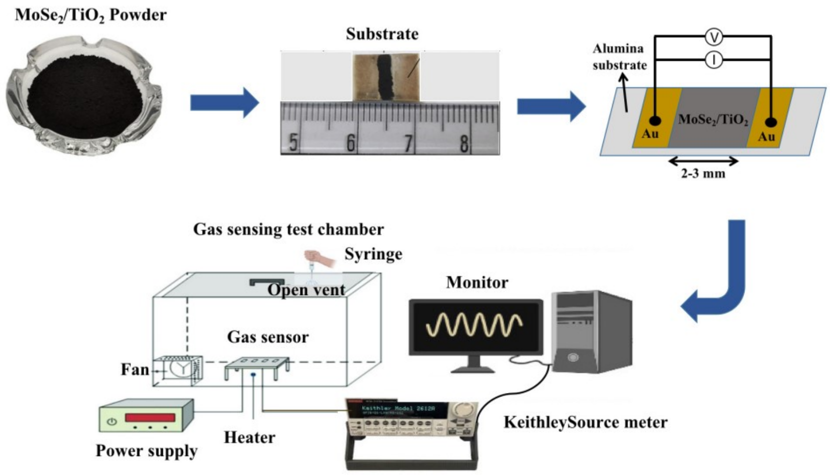

Figure S1: Schematic representation of sensing measurement geometry(a) $MoSe_2/TiO_2$ powder, (b-c) sensing device made from $MoSe_2/TiO_2$ composite and (d) gas sensing testing system.

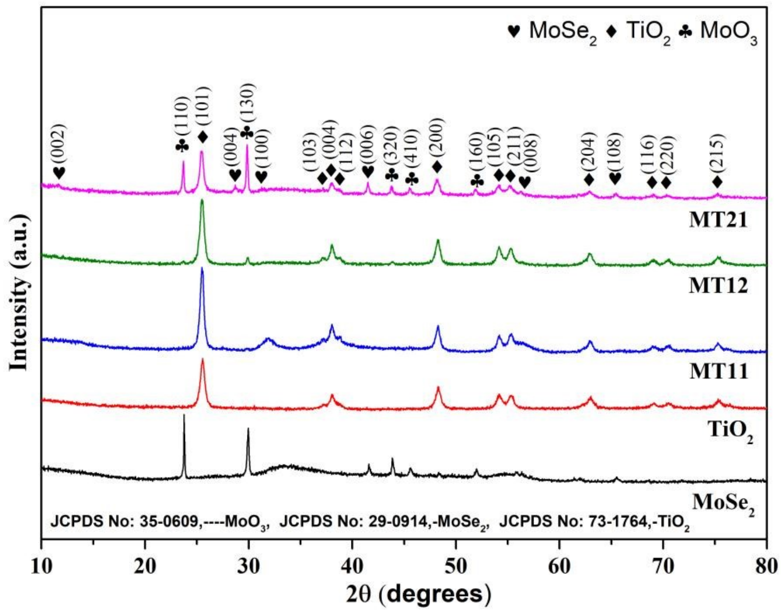

Figure S2: XRD pattern of $MoSe_2$, TiO_2 and $MoSe_2/TiO_2$ composite.

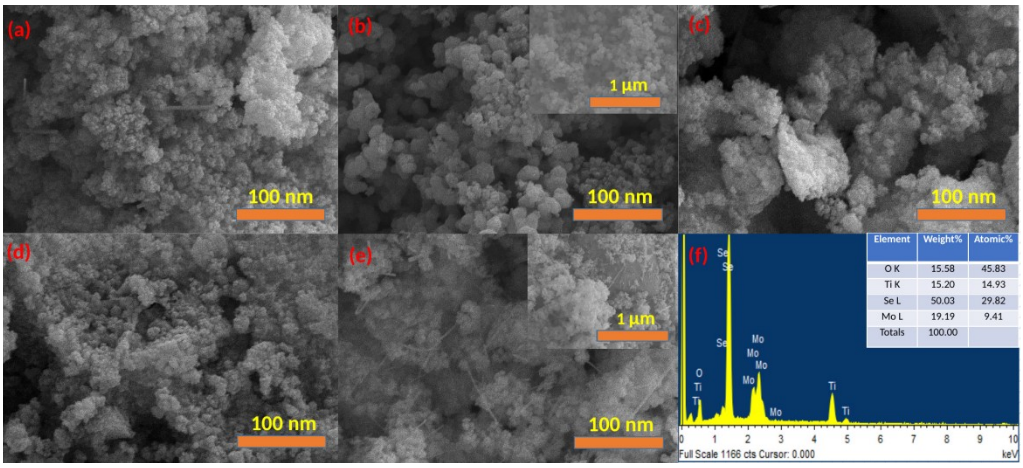

Figure S3: FESEM images of (a) $MoSe_2$, (b) TiO_2, (c) $MoSe_2/TiO_2$ (1:1) composite, (d) $MoSe_2/TiO_2$ (1:2) composite, (e) $MoSe_2/TiO_2$ (2:1) composite, (f) EDS pattern of $MoSe_2/TiO_2$ (2:1) composite.

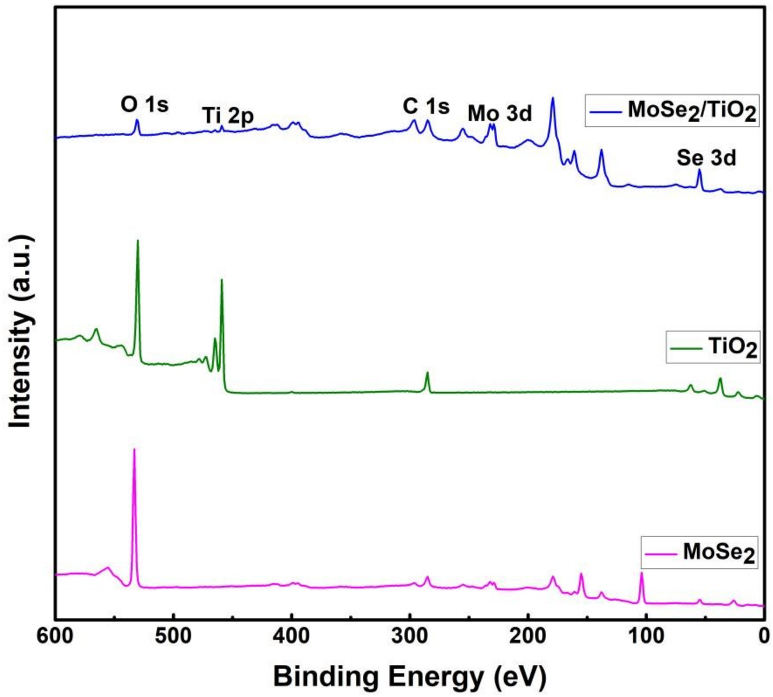

Figure S4: XPS survey spectrum of $MoSe_2$, TiO_2, and $MoSe_2/TiO_2$ (2:1) nanocomposite.

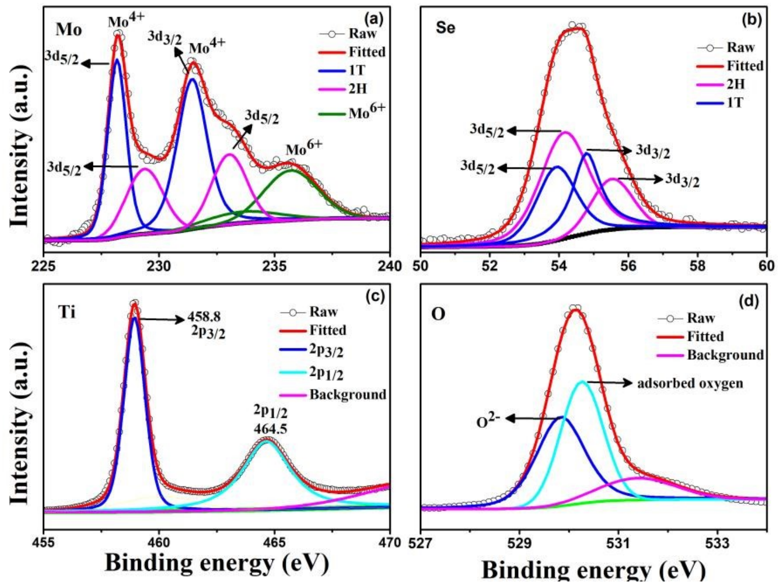

Figure S5: XPS spectra of $MoSe_2$ and TiO_2 (a) Mo 3d spectrum (b) Se 3d spectrum (c) Ti 2p spectrum, and (d) O 1s spectrum.

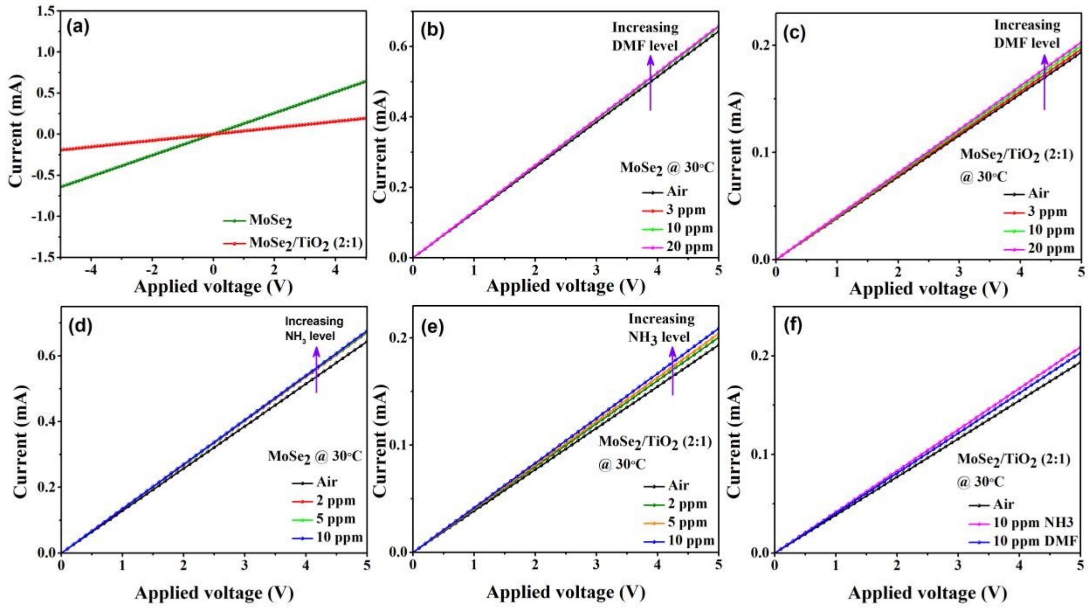

Figure S6: (a) IV measurements of $MoSe_2$, and $MoSe_2/TiO_2$ (2:1) composite sensors at 30 ℃ and 40% RH. (b) IV measurements of the $MoSe_2$ sensor in air and varying concentrations of DMF at 30 ℃and 40% RH. (c) IV measurements of the $MoSe_2/TiO_2$ (2:1) sensor in air and varying concentrations of DMF at 30 ℃ and 40% RH. (d) IV measurements of the $MoSe_2$ sensor in air and varying concentrations of NH_3 at 30 ℃ and 40% RH. (e) IV measurements of the $MoSe_2/TiO_2$ (2:1) sensor in air and varying concentrations of DMF at 30 ℃ and 40% RH. (f) IV measurements for $MoSe_2/TiO_2$ (2:1) composite sensor in air and 10 ppm of NH_3 or DMF.

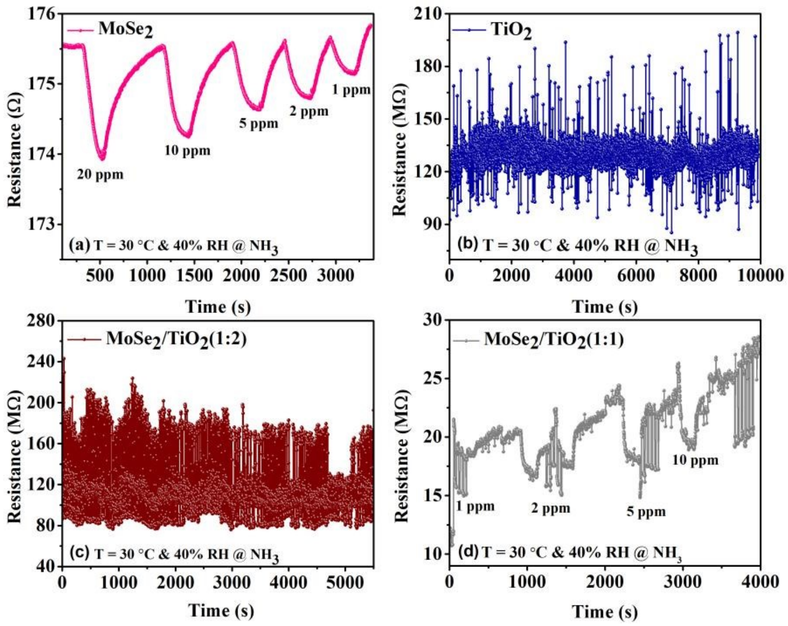

Figure S7: Different sensors upon exposure to different concentrations of NH_3. (a) $MoSe_2$, (b) TiO_2, (c) $MoSe_2/TiO_2$ (1:2), (d) $MoSe_2/TiO_2$ (1:1).

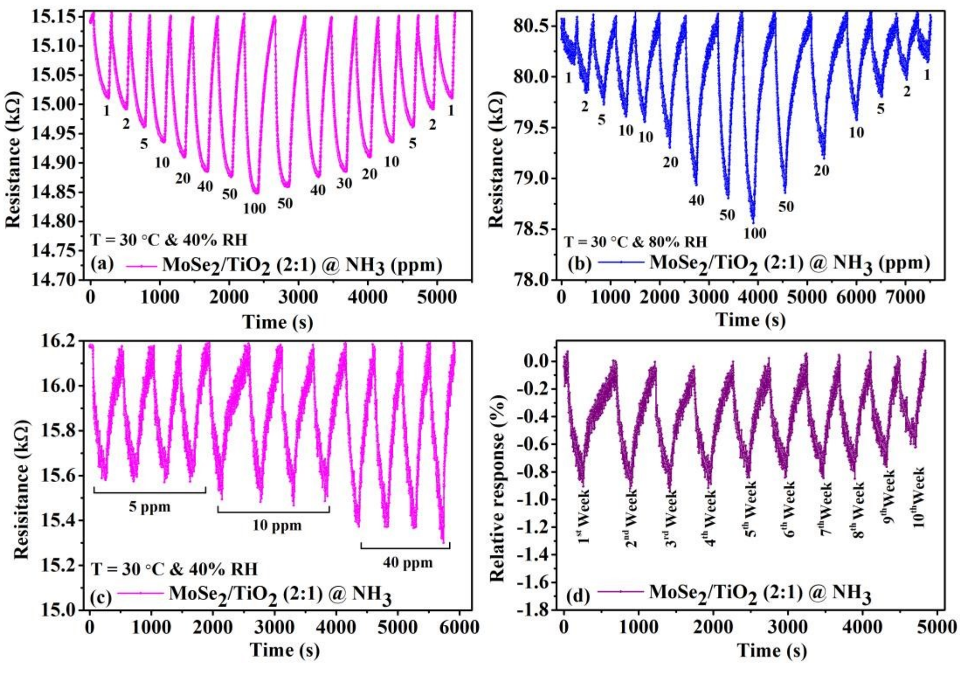

Figure S8: (a,b) Response transient curves for $MoSe_2/TiO_2$ (2:1) sensor upon exposure to different concentrations of NH_3 from 1 to 100 ppm at 30 ℃, 40% RH, and 80% RH. (c) Repeatability cycle test of $MoSe_2/TiO_2$ (2:1) sensor response to 5, 10, and 40 ppm of NH_3. (d) Long-term stability (10 weeks) of the $MoSe_2/TiO_2$ (2:1) sensor toward 10 ppm of NH_3.

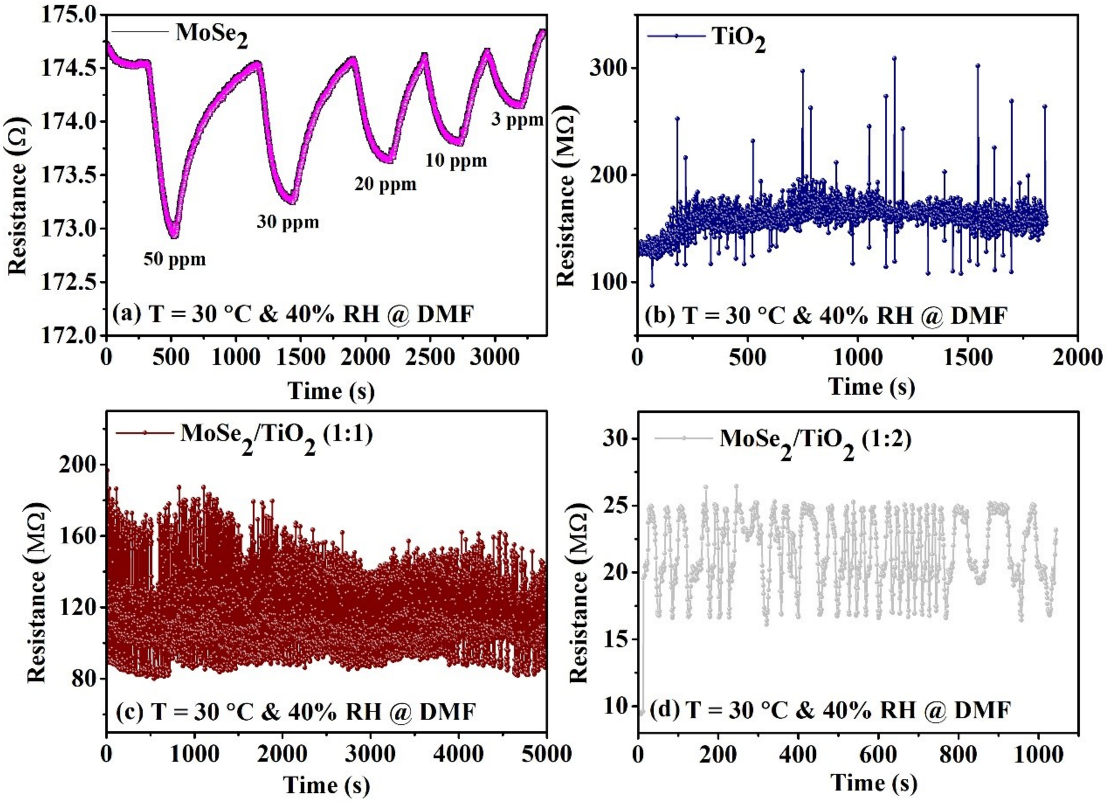

Figure S9: Different sensors upon exposure to different concentrations of DMF. (a) $MoSe_2$ (b) TiO_2 (c) $MoSe_2/TiO_2$ (1:2) (d) $MoSe_2/TiO_2$ (1:1).

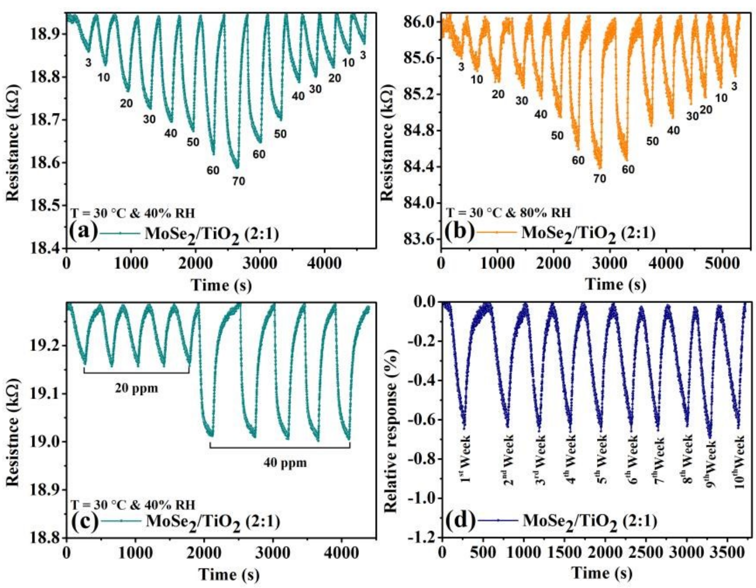

Figure S10: (a,b) Response transient curves for $MoSe_2/TiO_2$ (2:1) sensor upon exposure to different concentrations of DMF from 3 to 70 ppm at 30 ℃, 40% RH, and 80% RH. (c) Repeatability cycle test of $MoSe_2/TiO_2$ (2:1) sensor response to 20, and 40 ppm of DMF. (d) Long-term stability (10 weeks) of the $MoSe_2/TiO_2$ (2:1) sensor toward 10 ppm of DMF.

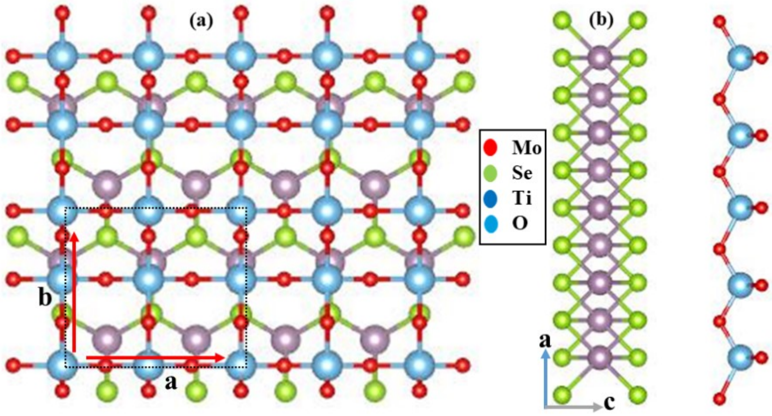

Figure S11:(a)Top and (b) side view of optimized $MoSe_2/TiO_2$ heterostructure.

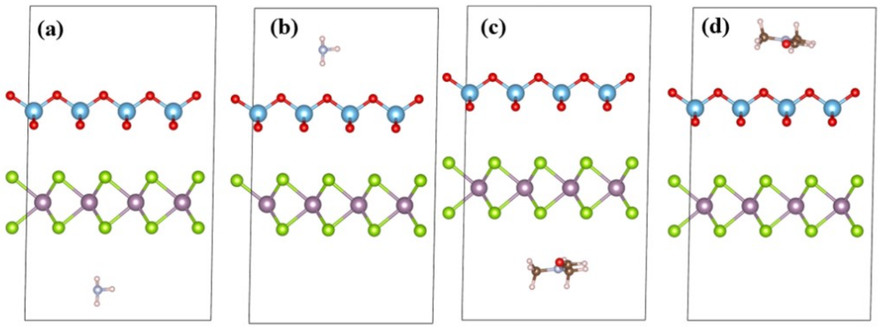

Figure S12:(a and c)below-$MoSe_2$ and (b and d)top-TiO_2 optimized structure after$NH_3$and DMF absorption on theheterostructure, respectively.

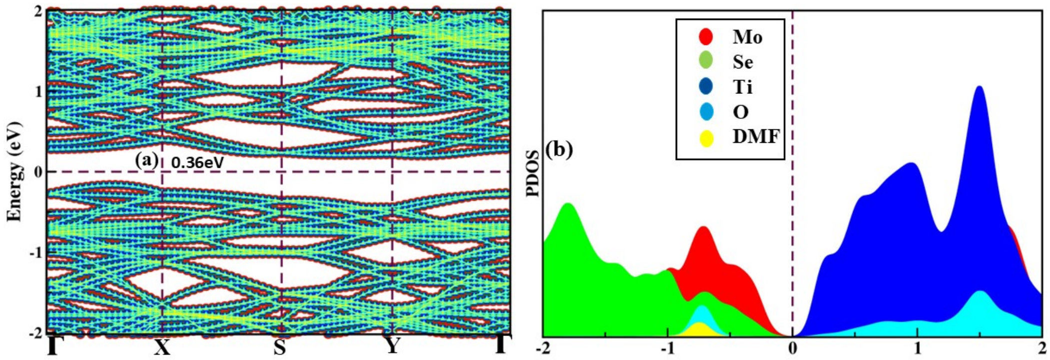

Figure S13: (a) and (b) Electronic band structure and Projected density of state of DMF adsorbed $MoSe_2/TiO_2$ heterostructure using GGA+PBE method.

References

1 S. Singh, R. Singh, S. S.-M. T. Proceedings and undefined 2020, Room temperature ammonia sensing using MoSe2 nanostructures, *ElsevierS Singh, RC Singh, S SharmaMaterials Today: Proceedings, 2020•Elsevier*.

2 D. Late, T. Doneux, M. B.-A. physics letters and undefined 2014, Single-layer MoSe2 based NH3 gas sensor, *pubs.aip.org*.

3 D. Zhang, Z. Yang, P. Li, M. Pang, Q. X.-N. Energy and undefined 2019, Flexible self-powered high-performance ammonia sensor based on Au-decorated MoSe2 nanoflowers driven by single layer MoS2-flake piezoelectric, *ElsevierD Zhang, Z Yang, P Li, M Pang, Q XueNano Energy, 2019•Elsevier*.

4 S. Y. Choi, Y. Kim, H. S. Chung, A. R. Kim, J. D. Kwon, J. Park, Y. L. Kim, S. H. Kwon, M. G. Hahm and B. Cho, Effect of Nb doping on chemical sensing performance of two-dimensional layered MoSe2, *ACS Appl Mater Interfaces*, 2017, **9**, 3817–3823.

5 P. Su, F. Chen, C. W.-S. and A. B. Chemical and undefined 2018, Simple one-pot polyol synthesis of Pd nanoparticles, TiO2 microrods and reduced graphene oxide ternary composite for sensing NH3 gas at room, *ElsevierPG Su, FY Chen, CH WeiSensors and Actuators B: Chemical, 2018•Elsevier*.

6 S. Sharma, A. Kumar, N. Singh and D. Kaur, Excellent room temperature ammonia gas sensing properties of n-MoS2/p-CuO heterojunction nanoworms, *Sens Actuators B Chem*, 2018, **275**, 499–507.

7 S. Singh, J. Deb, U. Sarkar and S. Sharma, MoS2/WO3Nanosheets for Detection of Ammonia, *ACS Appl Nano Mater*, 2021, **4**, 2594–2605.

8 Z. Qin, C. Ouyang, J. Zhang, L. Wan, S. Wang, C. Xie and D. Zeng, 2D WS2 nanosheets with TiO2 quantum dots decoration for high-performance ammonia gas sensing at room temperature, *Sens Actuators B Chem*, 2017, **253**, 1034–1042.

9 N. Dogra, S. S. Kushvaha and S. Sharma, Phase-Dependent Dual Discrimination of MoSe2/MoO3 Composites Toward N,N-Dimethylformamide and Triethylamine at Room Temperature, *ACS Sens*, 2023, **8**, 3146–3157.

10 N. Dogra and S. Sharma, Selective room-temperature dimethylformamide vapor sensing using MoSe2-rGO composite synthesized via facile hydrothermal method, *Mater Today Commun*, 2023, **35**, 106106.